

Synthesis and Characteristics of Nanoporous Carbon Spheres /S Composite as Cathode Material for Li-S Battery

Ping Liu¹, Wenhua Zhang², Ronghua Fang², Fayuan Wu¹, Liping Liu³, Qidong Kang²

¹ State Grid Jiangxi Electric Power Company Limited research institute, Minqiang Road No.88, 330096, Nanchang, China

² Nanchang Institute of Technology, Tianxiang Avenue No.289, 330099, Nanchang, China

³ Wuhan Guide Infrared Co., Ltd. Huanglongshan South Road No.6, 430205, Wuhan, China

*E-mail: 201594552@nit.edu.cn

Received: 25 January 2021 / Accepted: 12 March 2021 / Published: 31 May 2021

In this paper, three kinds of activated carbon microspheres with different particle size were prepared by hydrothermal method and carbon dioxide activation method by adjusting the concentration of sucrose solution (0.15M, 0.3M and 1.5M, respectively). Three kinds of composite materials, S-AMCS-0.15, S-AMCS-0.3 and S-AMCS-1.5, were prepared by the real air phase method, and the corresponding sulfur contents were 52%, 46% and 42%, respectively. The structure and morphology of various materials were characterized. The electrochemical properties of the three composites were investigated and compared. The experimental results show that S-AMCS-0.15 has good electrochemical performance. Due to the small particle size of AMCS-0.15 carbon microspheres, the active materials inside the spheres can be fully reacted. In order to further optimize the electrochemical properties of the composite, the material was treated by ball milling. The results show that the capacity retention and cycling properties of the composite have been improved to a certain extent. The discharge specific capacity in the second week also increased from 720 mAh g⁻¹ to more than 1180 mAh g⁻¹. And the discharge capacity maintained above 800 mAh g⁻¹ for the first 60 cycles.

Keywords: Li-S battery, nanoporous carbon spheres/S composite, cathode material

1. INTRODUCTION

Newly emerging technologies such as zero-emission electric vehicles (EVs) and advanced portable electronics impose an urgent demand on the next-generation rechargeable batteries with substantially increased energy density and significantly reduced cost. This demand has prompted the researches on lithium-sulfur (Li-S) batteries. Li-S batteries have high theoretical energy density (2600 Wh kg⁻¹) and competitive advantages of abundant availability, low price and environmental friendliness of sulfur, making it promising as an alternative of Li-ion batteries for large-scale applications[1-5].

However, fabricating sulfur cathode with high capacity and good cyclability encountered great challenges. The main reason is that the conventional sulfur electrode reaction is based on a solution-deposition mechanism and accompany with the generation of soluble polysulfide intermediates during the charge-discharge process. The dissolution of polysulfide ions in the electrolyte not only causes the diffusion loss of active material, the rapid increase of the electrolyte viscosity and the chemical corrosion of lithium anode, but also produces the "shuttle effect" of positive oxidation - negative reduction, leading to a fast capacity decay and a low coulomb efficiency at cycling[6-8].

The introduction of carbon-based materials as skeleton materials for sulfur composites has many advantages [9]. First, carbon materials have high electrical conductivity, which can well provide a conductive network for insulating sulfur and discharge product Li_2S , and improve the reaction kinetics of the positive electrode of sulfur. Secondly, carbon materials generally have rich pore structure, high specific surface area and excellent mechanical properties, which can effectively relieve the volume expansion of up to 80% in the process of charge and discharge. Thirdly, the nanopores of carbon material can inhibit the diffusion of soluble polysulfide ions to the electrolyte. According to the structure and morphology of carbon materials, they can be divided into zero-dimensional carbon spheres, one-dimensional carbon nanotubes, carbon fibers[10-13], two-dimensional graphene materials[14-16] and three-dimensional porous carbon materials[17-20].

We hypothesized that sulfur electrodes with high activity and cycling stability could be developed by using microporous carbon spheres as elemental sulfur carriers and organic carbonates insoluble electrolyte. Because microporous aperture small (< 2 nm), sulfur in highly dispersed in carbon microporous layer thickness is limited to a few molecules at most, can effectively avoid the insulation intermediate sulfur deposition caused by electrode deactivation, in this work, we prepared a series of microporous carbon ball and conductive for the carrier, the gas phase transfer of sulfur carbon composite materials, prepared by the electrochemical performance of sulfur carbon composites is examined, and on this basis, through the ball mill or adding a conductive agent to optimize its performance.

2. EXPERIMENTAL

2.1. Materials preparation

The specific preparation process of the microporous carbon sphere^[6] is as follows :(1) Preparation of Carbon ball precursor. 100mL sucrose aqueous solution with a certain concentration was prepared and transferred into PTFE tank in the hydrothermal reactor. The reactor was sealed and kept at 190°C for 5h, and then taken out when cooled to room temperature. The product was brown, washed with distilled water and filtered, and then dried overnight at 60 °C in vacuum to obtain the pre-carbonized product. (2) Carbonization of carbon ball. The pre-carbonized products were placed in a tubular furnace for carbonization at high temperature. Under the protection of high purity Ar, the pre-carbonized products were heated to 500 °C at 1 °Cmin⁻¹, then up to 1000 °C at 5 °C min⁻¹ and kept for 2h. The product was naturally cooled to room temperature, and then finely grounded for use. (3) Activation of

carbon sphere. The carbon spheres prepared above were placed in a CO₂ atmosphere and then heated to 800 °C at 5 °C min⁻¹ for 2 h to obtain activated carbon spheres.

The concentration of sucrose solution was 0.15 mol/L, 0.30 mol/L and 1.5 mol/L, respectively. The microporous carbon spheres were labeled as MCS-0.15, MCS-0.30 and MCS-1.5, respectively. The carbon carrier is activated in CO₂ atmosphere to increase pore volume. And the products were labeled as AMCS-0.15, AMCS-0.30 and AMCS-1.5.

Preparation of sulfur carbon composites: Activated microporous carbon spheres (AMCS) and elemental sulfur were placed in two sample bottles according to a certain mass ratio, and then placed in a closed reactor filled with argon gas, heated at 400°C for 6 h. According to the mass change of carbon material before and after heating, the mass percentage of sulfur in the composite material was calculated. S-AMCS-n (n=0.15, 0.30 and 1.5) was obtained by gas phase adsorption of activated microporous carbon spheres prepared with different concentrations of sucrose solution.

2.2 Structural characterization

The morphological and internal structural of the porous carbon and the S/C composite were examined by scanning electron microscope (SEM, Quanta 200, FEI, Netherlands), transmission electron microscopy (TEM, JEOL JEM-2010FEF, Japan electronics co., LTD). X-ray diffractometer (XRD-6000, Shimadzu, Cu K alpha, Shimadzu) was used to characterize the structure of carbon materials, as well as the distribution pattern of sulfur in the pores of carbon matrix. The scan range was 10 ° to 80 ° with a scan rate of 4 ° / min.

2.3 Electrochemical measurement

The sulfur cathode was prepared by mixing 80 wt.% S-AMCS composite material, 10 wt.% PTFE(polytetrafluoroethylene) and 10 wt.% acetylene black into a paste, and then roll-pressing the paste into about 0.1mm thick film, finally, pressing the prepared film onto an aluminum grid. The lithium sheet was used as counter electrode for the electrochemical tests of the prepared sulfur electrode in a CR2016 cell. 1 M LiPF₆/PC-EC-DEC (volume ratio of 1:4:5) was used as electrolyte.

The charge-discharge performance were achieved on a programmable computer-controlled battery charger (CT2001A Land Battery Testing System, Wuhan, China) by assembling 2016 type coin cells in the glove box (Mikrounasuperstar) filled with argon. The tests voltage range is 1.0~3.0 V and the current density is 100 mA g⁻¹.

3. RESULTS AND DISCUSSION SECTION

3.1 Structure and morphology characterization

Carbon dioxide activation was performed to increase the pore volume and specific surface area of the microporous carbon spheres. Figure 1 shows the SEM photos of the three kinds of microporous carbon spheres before and after activation. MCS-0.15(A), MCS-0.30(C), and MCS-1.5(E) are the

microporous carbon spheres synthesized by sucrose solution of 0.15M, 0.30M and 1.5M, and AMCS-0.30(D), MCS-1.5 (E) and AMCS-1.5(F) correspond to the electron microscope photos after activation respectively. As can be seen from the photo, the spherical structure of the four kinds of carbon microspheres is complete, and some microspheres have cross fusion. The particle size of the sphere is relatively uniform and the surface is smooth. Among them, the diameters of MCS-0.15, MCS-0.30 and MCS-1.5 are about 0.5 μm , 1 μm and 5 μm respectively. It can be seen that with the increase of sucrose solution concentration, the diameter of the microporous carbon spheres increased gradually.

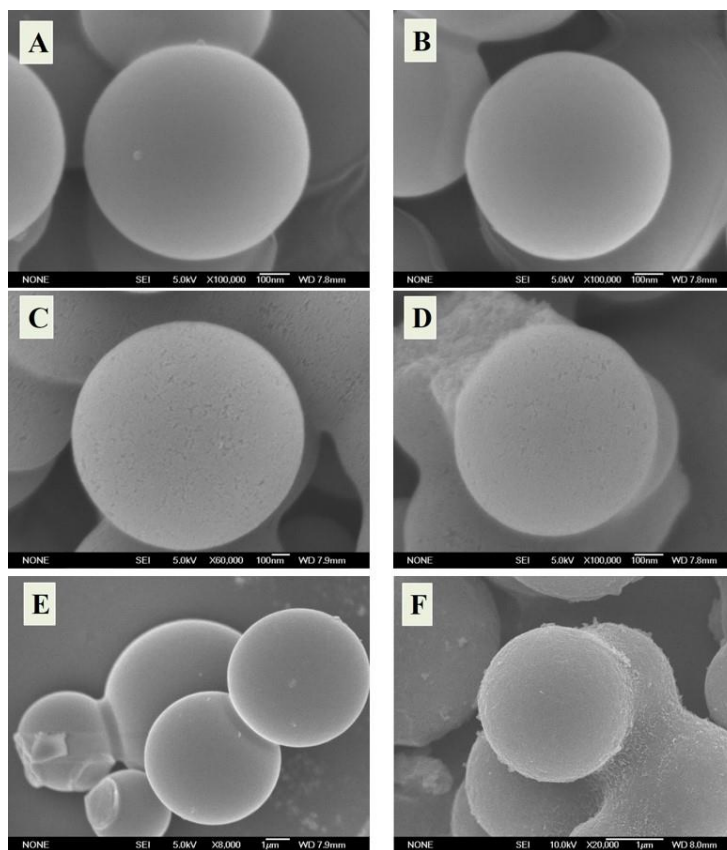


Figure 1. SEM photographs of microporous carbon spheres synthesized by sucrose solution with different concentrations before and after activation MCS-0.15 (A), AMCS-0.15(B), MCS-0.30 (C), AMCS-0.30(D), MCS-1.5 (E), and AMCS-1.5(F)

After activation, the spherical structure and size of the microspheres has not change significantly, and the surface of the spheres became slightly rough, indicating that carbon dioxide activation could increase the specific surface area of the carbon microspheres. This phenomenon is consistent with the results in reference[21]. Table 1 shows the specific surface area and pore structure parameters of three kinds of microporous carbon spheres determined by static nitrogen adsorption method. The data in the table show that with the increase of sucrose solution concentration, the specific surface area of the microporous carbon sphere decreases gradually, and the pore volume and pore diameter of the

microporous carbon sphere also decrease. This may be because the higher the concentration of sucrose solution, the tighter the arrangement of sucrose molecules during dehydration and polymerization to form spherical micelles, and the smaller the pores formed[22]. After activation, the specific surface area and pore structure parameters of the microporous carbon sphere were increased correspondingly. Among them, MCS-0.15 carbon microsphere showed the greatest change, which may be due to its smaller particle size and higher reaction rate of carbon dioxide on the surface and pore wall of the carbon sphere[23].

Table 1. Specific surface area and pore structure parameters of the microporous carbon sphere

The sample	Specific surface area ($\text{m}^2 \text{g}^{-1}$)	Pore volume ($\text{cm}^3 \text{g}^{-1}$)	The average pore diameter (nm)
MCS-0.15	840.2	0.33	0.99
MCS-0.30	781.8	0.30	0.85
MCS-1.5	299.0	0.12	0.75
AMCS-0.15	1551	2.39	1.34
AMCS-0.30	1214	2.74	1.08
AMCS-1.5	1026	1.02	0.98

AMCS-0.15 was selected as the representative, and the apparent morphology of the composite sulfur was observed by high resolution transmission electron microscopy (HRTEM). Large number of nanopores with a diameter of ~ 1 nm were distributed inside the microporous carbon spheres before sulfur recombination as shown in Figure 2(a). Such a well-developed nanopore structure can provide a large number of channels for elemental sulfur to enter the carbon microsphere. However, in Figure 2(b), after sulfur recombination, no obvious morphological differences were observed, indicating that almost all the elemental sulfur in the S-AMCS-0.15 composite was embedded in the nano-pore of the carbon microspheres, and was not deposited on the outer surface of the carbon material or in the spherical interstice[24].

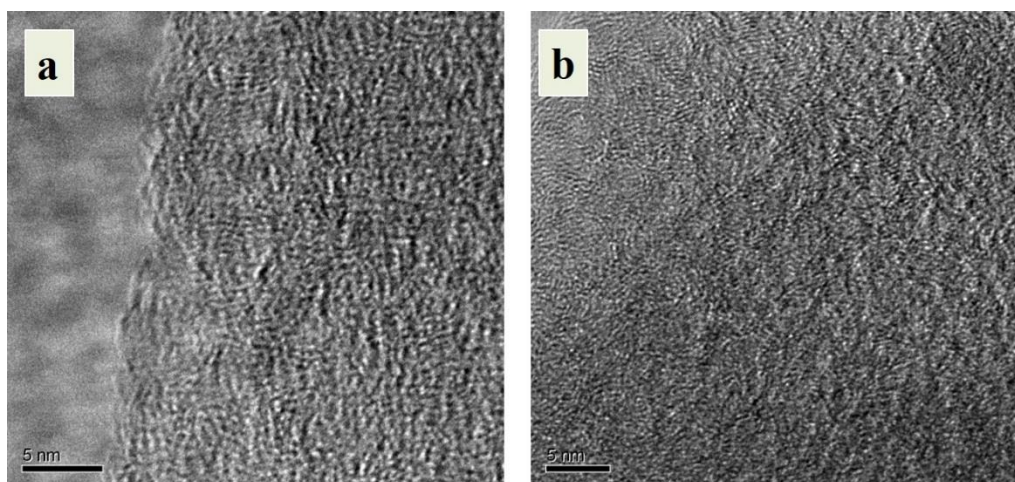


Figure 2. HRTEM images of AMCS-0.15 carbon microspheres before and after sulfur recombination. a) before recombination, b) after recombination.

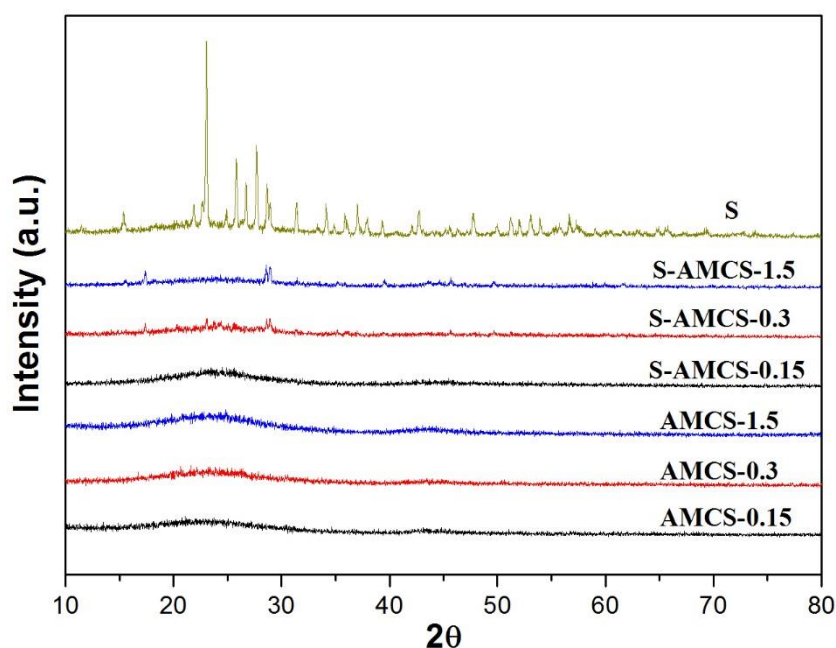


Figure 3. XRD patterns of activation of microporous carbon spheres before and after impregnating sulfur

Figure 3 shows the XRD patterns of activated microporous carbon spheres before and after sulfur recombination. It can be seen that the spectrograms of AMCS-0.15, AMCS-0.3 and AMCS-1.5 microporous carbon spheres are basically the same, and there are two broad graphite diffraction peaks around $\sim 23^\circ$ and $\sim 44^\circ$ respectively. The low peak strength indicates that the carbon matrix of microspheres is amorphous carbon structure. The XRD patterns of the sublimated sulfur show sharp diffraction peaks, indicating that the sublimated sulfur exists in crystalline form. However, in the XRD pattern of S-AMCS-0.15 composite material, only the weak broad diffraction peak corresponding to the carbon matrix is found, showing that the elemental sulfur is highly dispersed in the pores of the carbon

matrix in the size of nanometer or sub-nanometer. In the XRD patterns of S-AMCS-0.3 and S-AMCS-1.5 composites, the two broad diffraction peaks corresponding to the carbon material become weaker, and a small number of characteristic peaks corresponding to sulfur appear. These indicate that in the S-AMCS-0.3 and S-AMCS-1.5 composites, elemental sulfur is not only filled in the pores of the carbon matrix, but also distributed on the surface of the carbon sphere[24].

3.2 Electrochemical properties

Figure 4 shows the charge and discharge curves of three kinds of S-AMCS composite materials in 1M LiPF₆/PC-EC-DEC electrolyte. Among them, the S-AMCS-0.15 composite with sulfur content of 52% only showed a platform of ~1.65V in the first discharge cycle, with specific discharge capacity of about 1120mAhg⁻¹. In the subsequent charging process, the voltage platform was located near ~2.0V, and the charging capacity was about 700mAhg⁻¹. As the cycle goes on, the polarization of the charging and discharging platform decreased. After 50 cycles, the capacity remained at about 550mAhg⁻¹. For the S-AMCS-0.30 composite material with sulfur content of 46%, a voltage platform at 1.65V appeared in the first discharge cycle. In the subsequent charging process, the voltage platform was located near ~2.0V. As the cycle goes on, both the charging and discharging voltage platforms increased, and the discharge capacity remained above 400mAhg⁻¹ after 100 cycles. For the S-AMCS-1.5 composite material with sulfur content of 42%, two voltage platforms at 2.35V and 1.8V appeared in the first discharge cycle. Among them, the capacity of the platform located at 2.35V was only about 50mAhg⁻¹, and the main discharge capacity was concentrated in the 1.8V platform. In the subsequent charging process, a single charging platform appeared above 2.0V, without a charging voltage platform corresponding to the 2.35V high-potential discharge platform. Moreover, the high-potential discharge platform completely disappeared after the first cycle, indicating that the discharge corresponding to 2.35V was an irreversible reduction of sulfur[d]. Combined with the previous XRD characterization, it can be seen that in the S-AMCS-1.5 material with sulfur content of 42%, there is a small amount of elemental sulfur on the surface of the carbon microspheres. Therefore, the high-voltage platform during the first-cycle discharge should be irreversibly reduced on the surface of the carbon microspheres. During the first cycle, the discharge capacity of the composite material is 1600mAhg⁻¹, while the charging capacity is only 1100mAhg⁻¹. After 40 cycles, the capacity remained above 600 mAhg⁻¹. Comparing the electrochemical properties of the three materials, it is easy to find that the S-AMCS-0.15 composite material has a higher capacity retention rate and cycling performance, due to the small diameter of the AMCS-0.15 carbon microsphere, which can make the active material inside the sphere fully react. Although most of the composite sulfur electrodes with microporous carbon spheres as carriers showed excellent cyclic stability, their circulating capacity was generally low at about 500 mAhg⁻¹. There are two possible reasons for this phenomenon: (1) The carbon microsphere has a large particle size and porous, the electron transport path inside the sphere is long and difficult to transfer, and the active substances embedded in deeper pores are difficult to participate in the reaction, leading to a low utilization of the active substances. (2) The presence of a small amount of sulfur elemental substance on the surface of the carbon sphere and the re-deposition of a small amount of dissolved lithium polysulfide

on the carbon surface during the charging process partially cut off the electronic transmission between the composite materials[25]. These results in the inactivation of part of the material and the reduction of reversible capacity[4]. If the spheres size can be reduced and the electrical contact between spheres in the composite material can be improved, it is possible to improve the specific capacity of the material. Therefore, we chose S-AMCS-0.15 composite material with better performance and processed it after ball grinding. Under the protection of nitrogen, the star grinding was carried out for 6h.

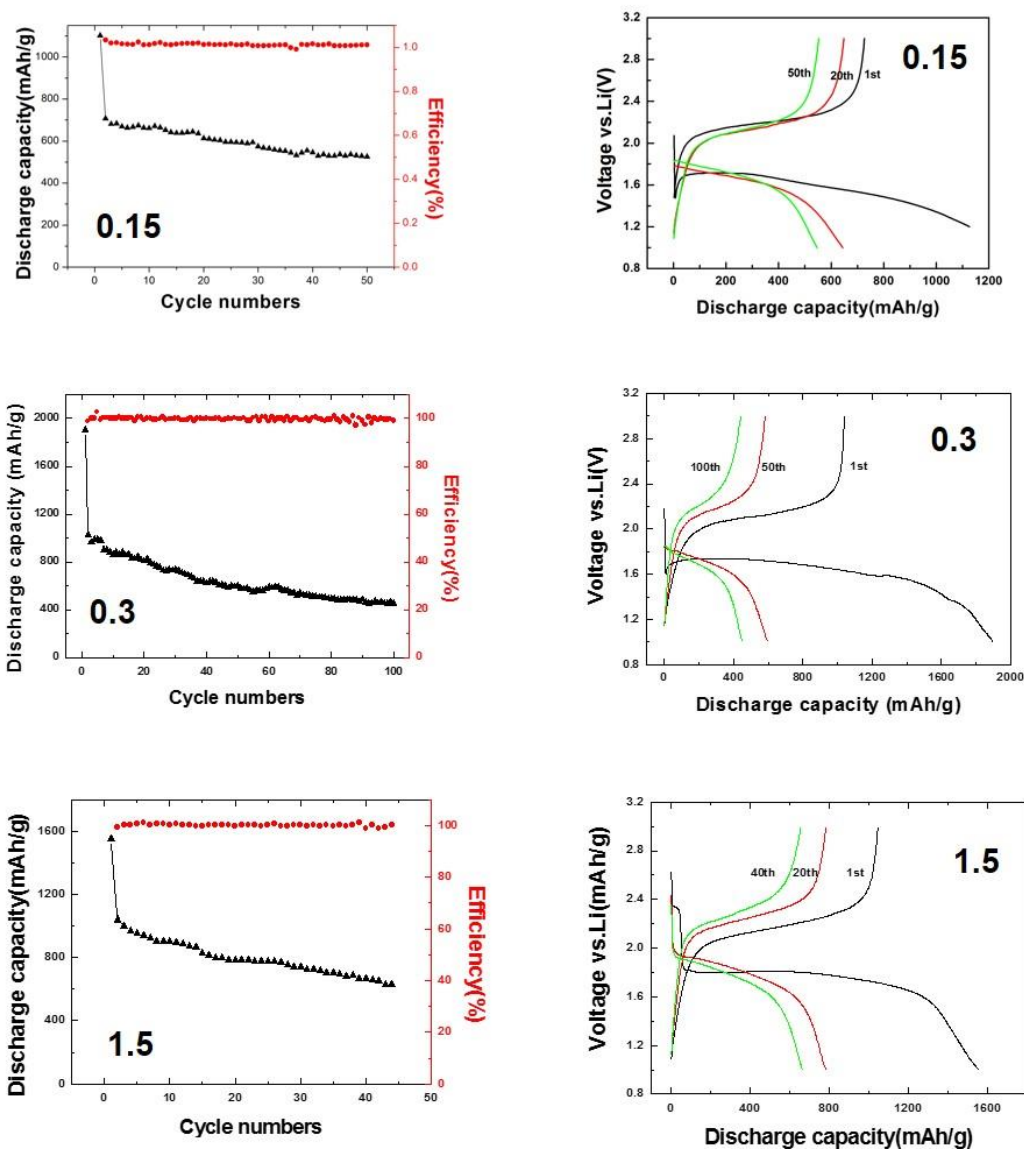


Figure 4. Charge-discharge curve and cycle curve of S-AMCS composite in 1M LiPF₆/PC-EC-DEC electrolyte, current density: 100 mA h⁻¹, voltage range: 1.0~ 3.0V

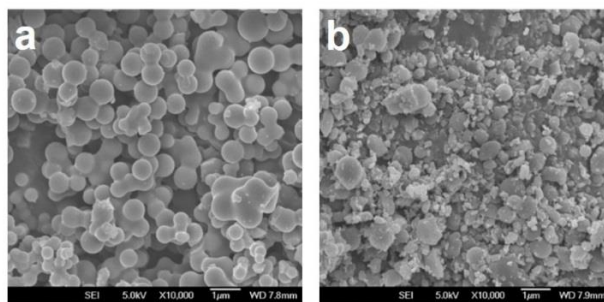


Figure 5. S-AMCS-0.15 SEM photos of sulfur-carbon composite material before and after ball grinding, before ball grinding (a), after ball grinding (b)

In order to improve the capacity of sulfur carbon composites, the material was ground to make its particle size smaller. Scanning electron microscopy (SEM) was used to observe the morphology changes of the S-AMCS-0.15 composites prepared before and after ball milling, and the results were shown in Figure 5. It can be seen that the spherical structure of S-AMCS-0.15 composite material is completely destroyed after the ball milling treatment. Before milling, it is composed of dispersed complete spheres with particle size of ~ 500 nm. After grinding, most of the spheres were destroyed and transformed into small fragments with particle sizes of 200–300 nm. The results show that the particle size of the sulfur-carbon composite material is greatly reduced by ball-milling.

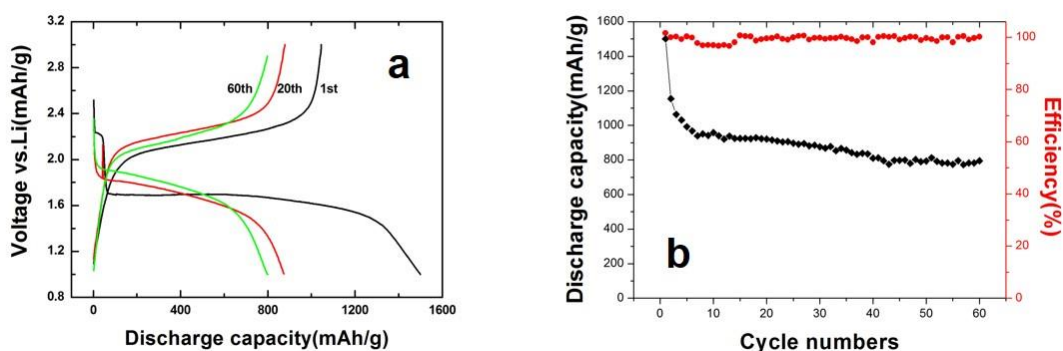


Figure 6. The charging-discharging performance (a) and cycling performance(b) of S-AMCS-0.15 composite material after ball milling

In addition, we further investigated the charging-discharging performance and cycling performance of S-AMCS-0.15 composite material after ball milling. As shown in figure 6(a), both the discharging platform and the charging platform were increased after ball milling. In the first discharge cycle, two voltage platforms appeared at ~ 2.3 V and ~ 1.7 V, while the capacity of the platform located at 2.3 V was only about 100 mAhg^{-1} , and the capacity mainly concentrated on the 1.7 V voltage platform. In the subsequent charging process, only a single charging platform appeared above 2.0 V, without a charging voltage platform corresponding to the 2.3 V high-potential discharge platform. Moreover, the high-potential discharge platform completely disappeared after the first discharge cycle, indicating that the discharge corresponding to 2.3 V refer to the irreversible reduction of sulfur. The possible reason was that with the pulverization of the spheres during ball grinding, a large number of bulk phase holes were

destroyed and exposed to the electrolyte, making the original partial bulk phase sulfur become surface sulfur. Figure 6 (b) showed that the discharge specific capacity of S-AMCS-0.15 composite material after ball grinding also increased from 720 mAhg⁻¹ to over 1180 mAhg⁻¹ in the second cycle. In the first 60 cycles, the discharge capacity maintained above 800 mAhg⁻¹, and the capacity retention rate was 54.0%. Before ball milling, the discharge capacity after 50 cycles was only 550 mAhg⁻¹, and the capacity retention rate was 46.7%. The results show that the capacity retention rate and cycling performance of the composite had been improved after the treatment of ball milling. The reason was that the utilization rate of the active material increases significantly with the breaking of the spherical structure and the decrease of the carbon matrix size[24].

Table 2. Comparison of electrochemical performance of the prepared sulfur electrodes

Cathode	Sulfur loading (wt%)	Initial discharge capacity(mAhg ⁻¹)	Stable discharge capacity after 60 cycles(mAhg ⁻¹)	Rate (mAhg ⁻¹)	Reference
Microporous carbon sphere /S (S-AMCS-0.15)	52%	1180	800	100	This work
Acetylene black/S	36%	934.9	500	40	[26]

Table 2 compared the performance of microporous carbon sphere /S composites (S-AMCS-0.15) prepared in this work and the Acetylene black /S reported in the literature [26]. Acetylene black/S with 36% sulfur has a stabilized discharge capacity of 500mAh/g after the 50th cycle. The discharge capacity of S-AMCS-0.15 composite is 1180 mAhg⁻¹ in first cycle and 800 mAhg⁻¹ after 60 cycles. However, The discharge capacity of Hollow carbon sphere/S composite is 1445 mAhg⁻¹ in first cycle and 750 mAhg⁻¹ after 100 cycles. This is mainly due to the treatment of ball milling of S-AMCS-0.15 can reduce particle size and provide more S/e/Li⁺ three-phase reaction sites for the composite. And the . It shows that microporous carbon sphere /S has better electrochemical performance.

4. CONCLUSION

In this paper, three kinds of activated carbon microspheres with different particle sizes were prepared by hydrothermal method and carbon dioxide activation method by adjusting the concentration of sucrose solution (0.15 M, 0.3 M and 1.5 M, respectively), and three kinds of composite materials, S-AMCS-0.15, S-AMCS-0.3 and S-AMCS-1.5, were prepared by vacuum phase method. The corresponding sulfur content was 52%, 46% and 42%, respectively. The structure and morphology of various materials were characterized, and the electrochemical properties of three kinds of composites were investigated and compared. The experimental results revealed that S-AMCS-0.15 showed good electrochemical performance. Due to the small particle size of AMCS-0.15 carbon microspheres, the active materials inside the spheres can be fully reacted. In order to further optimize the electrochemical

properties of the composite, the material was treated by ball milling. The results showed that the capacity retention and cycling properties of the composite had been improved to a certain extent.

ACKNOWLEDGEMENTS

This work was supported by Project of State Grid Jiangxi Electric Power Co., LTD. [52182018000S], the National Natural Science Foundation of China [grant number 21603093, 21702090].

References

1. P.G. Bruce, S.A. Freunberger, L.J. Hardwick, *Nat. Mater.*, 11 (2012) 19.
2. Y.V. Mikhaylik, J.R. Akridge. *J. Electrochem. Soc.*, 11(2004) A1969.
3. J.M. Tarascon, M. Armand, *Nature*, 414(2001) 359.
4. A. Manthiram, Y.Fu, S.H. Chung, C. Zu, Y.S. Su, *Chem. Rev.*, 114 (2014) 11751.
5. J. Conder, C. Villevieille, *Curr. Opin. Electrochem.*, 9 (2018) 33.
6. Y. Y. Yan, C. Cheng, L. Zhang, *Adv. Energy Mater.*, 18(2019) 1900148.
7. L. Zhang, T. Qian, X. Y. Zhu, *Chem. Soc. Rev.*, 22 (2019) 5432.
8. J. J. Chen, R. M. Yuan, J. M. Feng, *Chem. Mater.*, 27(2015) 2048.
9. Z.W. Seh, Y. Sun, Q. Zhang, Y. Cui, *Chem. Soc. Rev.*, 45 (2016) 5605.
10. Q. Li, Z. Zhang, Z. Guo, K. Zhang, Y. Lai, J. Li, *J. Power Sources*, 274(2015) 338.
11. L. Sun, M.Li, Y. Jiang, W. Kong, K. Jiang, J. Wang, S. Fan, *Nano Lett.*, 14 (2014) 4044.
12. L. Ji, M. Rao, S. Aloni, L. Wang, E.J. Cairns, Y. Zhang, *Energy Environ. Sci.*, 4 (2011) 5053.
13. Y.B. Yang, H. Xu, S.X. Wang, Y.F. Deng, X.Y. Qin, *Electrochim. Acta*, 297 (2019) 641.
14. Y. Qiu, W. Li, W. Zhao, G. Li, Y. Hou, M. Liu, L. Zhou, F. Ye, H. Li, Z. Wei, S. Yang, W. Duan, Y. Ye, J. Guo, Y. Zhang, *Nano Lett.*, 14 (2014) 4821.
15. X.D. Hong, J. Liang, X.N. Tang, H.C. Yang, F. Li, *Chem. Eng. Sci.*, 194 (2019) 148.
16. S.X. Jia, X.P.Chen, F. Ping, Z.P. Zhao, F. Chen, M.Q. Zhong, *Int. J. Electrochem. Sci.*, 13 (2018) 3407.
17. B. Zhang, X. Qin, G.R. Li, X.P. Gao, *Energy Environ. Sci.*, 3 (2010) 1531.
18. W.H. Zhang, D. Qiao, J.X. Pan, Y.L. Cao, H.X. Yang, X.P. Ai, *Electrochim. Acta*, 87 (2013) 497.
19. X.L. Ji, K.T. Lee, L.F. Nazar, *Nat. Mater.*, 8 (2009) 500.
20. J. Song, T. Xu, M.L. Gordin, P. Zhu, D. Lv, Y.B. Jiang, Y. Chen, Y. Yuan, D. Wang, *Adv. Funct. Mater.*, 24 (2014) 1243.
21. Y.G. Lu, C.L. Yang, H.Q. Rong, D. Pan, *Journal of Applied Polymer Science*, 102(2006) 798–803.
22. E.R. Buiel, A.E. George, J.R. Dahn, *Carbon.*, 37 (1999) 1399–1407.
23. H. Teng, S.C. Wang, *Carbon.*, 38 (2000) 817–824
24. W.H. Zhang, D. Qiao, J.X. Pan, Y.L. Cao, H.X. Yang, X.P. Ai, *Electrochimica Acta.*, 87 (2013) 497– 502.
25. W.H. Zhang, P. Liu, J.X. Pan, X.P. Yang, J. Liu, H.J. Xu, Z.Z. Ouyang, *Int. J. Electrochem. Sci.*, 14 (2019) 4693 – 4704
26. B. Zhang, C. Lai, Z. Zhou, X.P. Gao, *Electrochimica Acta.*, 54 (2009) 3708–3713